Journal of Mass Spectrometry and Advances in the Clinical Lab 22 (2021) 50–55

Contents lists available at ScienceDirect

Journal of Mass Spectrometry and Advances in the Clinical Lab

journal homepage: www.sciencedirect.com/journal/journal-of-mass-spectrometry-and-advances-in-the-clinical-lab

The effect of sample age on the metabolic information extracted from formalin-fixed and paraffin embedded tissue samples using desorption electrospray ionization mass spectrometry imaging☆

Olof Gerdur Isberg [a,b,c,*], Yuchen Xiang [a], Sigridur Klara Bodvarsdottir [c], Jon Gunnlaugur Jonasson [d,e], Margret Thorsteinsdottir [b,c], Zoltan Takats [a,1]

[a] Department of Metabolism, Digestion and Reproduction, Faculty of Medicine, Imperial College London, London SW7 2AZ, United Kingdom
[b] Faculty of Pharmaceutical Sciences, University of Iceland, Hofsvallagata 53, 107 Reykjavik, Iceland
[c] Biomedical Center, University of Iceland, Reykjavik, Iceland
[d] Pathology, Landspitali-National University Hospital, Reykjavik, Iceland
[e] Faculty of Medicine, University of Iceland, Reykjavik, Iceland

ARTICLE INFO

Keywords:
Sample age
Lipids
DESI-MSI
FFPE
Mass spectrometry imaging

ABSTRACT

Background: Metabolites, especially lipids, have been shown to be promising therapeutic targets. In conjugation with genes and proteins they can be used to identify phenotypes of disease and support the development of targeted treatments. The majority of clinically collected tissue samples are stored in formalin-fixed and paraffin embedded (FFPE) blocks due to their tissue conservation ability and indefinite storage capacity. For metabolic analysis, however, fresh frozen (FF) samples are currently preferred over FFPE samples due to concerns of metabolic information being lost when preparing the samples. With little or no sample preparation, desorption electrospray ionisation mass spectrometry imaging (DESI-MSI) allows for the study of spatial as well as spectral information.

Methods: DESI-MSI analysis was performed on FFPE breast cancer tissue microarray samples from 213 patients collected between the years 1935-2013. Logistic regression (LR) models were built to classify samples based on age and FF samples were used for feature validation.

Results: LR models developed on the FFPE samples achieved an average classification accuracy of 96% when predicting their age with a 10-year grouping. Closer examination of the metabolic change over time revealed that the mean signal intensities for the lower mass range (100 - 500 m/z) linearly decrease over time, while the mean intensities for the higher mass range (500 - 900 m/z), remained relatively constant.

Conclusions: In our samples, which span over 70 years, sample age has a weak yet quantifiable impact on metabolite content in FFPE samples, while the higher mass range is seemingly unaffected. FFPE samples thus provide an alternative avenue for metabolic analysis of lipids.

1. Introduction

Metabolites are small molecular products or substrates of metabolic processes that play a critical role in a variety of cellular functions [1,2]. They can be divided into multiple classes including nucleotides, sugars, and lipids [3–5], serving different biological functions, such as energy sources or signal transducers for regulatory processes by interacting with proteins. In particular, lipids are essential components of biological membranes [4,6–8]. Along with genes and proteins, metabolites can be a powerful tool for identifying disease phenotypes, placing metabolomics at the forefront of pathological biomarker discovery [1–4]. Numerous human diseases such as cancer, diabetes and neurodegenerative

☆ This document is the result of the research project funded by the Icelandic Centre for Research, grant no. 174566051 and by the Icelandic Breast Cancer Research Fund, Göngum Saman.

* Corresponding author at: Department of Metabolism, Digestion and Reproduction, Faculty of Medicine, Imperial College London, London SW7 2AZ, United Kingdom.
E-mail addresses: o.isberg18@imperial.ac.uk (O.G. Isberg), z.takats@imperial.ac.uk (Z. Takats).
[1] Principal corresponding author.

https://doi.org/10.1016/j.jmsacl.2021.10.004

Available online 28 October 2021

pathologies, exhibit lipid homeostasis imbalance, making lipids essential therapeutic research targets [8,9]. Metabolites have often been difficult to analyse due to their chemical complexity and variety, but in recent years, metabolomics has emerged as one of the most rapidly developing and evolving fields. This is largely due to the advances in the field of mass spectrometry (MS) [6,9].

Mass spectrometry has been widely used in metabolic research. MS is especially appealing because of its speed of analysis, and its use in conjunction with separation techniques, such as liquid chromatography, gas chromatography, and ion mobility analysis [8,10,11]. With its high sensitivity, MS can provide extensive metabolomic coverage, however, consistency in preparation, handling and storage of samples is critical [10,11]. Existing literature has yet to quantitatively demonstrate the impact of sample preparation and storage conditions on metabolic-relevant spectral details. Several ambient ionisation MS techniques have been introduced that require little or no sample preparation, with desorption electrospray ionisation mass spectrometry (DESI-MS) being one of them [10,12].

The integration of sample scanning and DESI-MS imaging (together called MSI) allows the investigation of the spatial distribution of a wide range of molecules in biological samples providing crucial knowledge of biological processes occurring within tissues [13,14]. For clinical studies, DESI-MSI analysis has been shown to be both reproducible and repeatable [15]. Furthermore, DESI-MSI has also shown great potential in analysing different forms of fresh frozen (FF) cancer tissues, including breast [16–18], ovarian [19,20], and colorectal [21,22].

In existing metabolomics workflows, FF samples have traditionally been preferred over formalin-fixed and paraffin embedded (FFPE) samples due to concerns with metabolite changes in FFPE samples. However, recent studies have shown that FFPE samples still contain useful biochemical information [23–27]. Currently, the majority of clinically obtained tissue samples are processed as FFPE samples due to its tissue preservation ability [28]. Worldwide, FFPE encompasses vast repositories of clinical samples spanning decades. Unsurprisingly, these samples have drawn interest due to the tremendous amount of clinical information that they may still contain [24,27,28]. Moreover, compared with FF samples, FFPE samples undergo minimal tissue degradation, and can be stored at room temperature, making FFPE samples ideal for a convenient and cost-effective workflow [29]. Therefore, FFPE samples are extremely valuable resources for clinical research [24,28,29]. Despite the clear attraction that the FFPE sample bank presents, particular care must be taken when extracting information from these long-storage samples. Namely, the age of the sample may affect the metabolic information over time. In this study, with a clinical dataset spanning over 70 years, we explore the possible effect of sample age using data analytical approaches and present qualitative results based on predictive modelling of the impact of sample age on metabolomic content in FFPE samples.

2. Materials and methods

2.1. Sample preparation

Human FFPE breast cancer tissue microarrays (TMA) and FF breast cancer tissue samples were obtained from the Department of Pathology, Landspitali Hospital in Iceland (Reykjavik, Iceland). A total of 9 FFPE TMA blocks were prepared including 583 breast cancer tissue cores from 213 patients (1–6 cores from each patient) diagnosed from 1935 to 2013 [30]. Each TMA FFPE slide includes a kidney and a liver core as control, the former was used to scale the data to avoid inter-run batch effect (Section 2.3). Fresh frozen breast cancer tissue samples and adjacent normal breast tissue samples from 44 individuals collected in the years of 1990-2003 were hydrogel-embedded [31] into TMA blocks (n = 7) and stored at −80 °C. The FF TMAs were cryosectioned to 12 μm thickness and stored in −80 °C. The study was approved by the Icelandic Bioethics Committee (reference number: VSNb2017030012-03.03) and was carried out in accordance with The Code of Ethics of the World Medical Association (Declaration of Helsinki) for experiments involving humans:https://www.wma.net/policies-post/wma-declaration-of-helsinki-ethical-principles-for-medical-research-involving-human-subjects/.

2.2. DESI-MSI analysis

Tissue samples were analysed using a Xevo G2-XS QTOF mass spectrometer (Waters Corporation, Milford, MA, USA) controlled by MassLynx 4.1 software (Waters Corporation, Milford, MA, USA) in negative ion mode with mass range 50 - 1000 m/z. The mass spectrometer was coupled to a two-dimensional DESI stage from Prosolia Inc. (Indianapolis, IN, USA) and set at a spatial resolution of 85 μm. The instrumental parameters can be seen in Supplementary Table 1. FFPE samples were deparaffinized prior to DESI-MSI analysis by incubating the samples for 1 h at 60 °C, rinsing with xylene (2 × 8 min) and air-drying in a fume-hood overnight [26]. Following DESI-MSI analysis, FFPE TMAs were stained with haematoxylin and eosin (H&E) and scanned with a high-resolution digital slide scanner (NanoZoomer2.0-HT, Hamamatsu City, Japan). Consecutive samples were H&E stained due to the deterioration of the analysed tissue.

2.3. Data analysis

Data pre-processing was first performed on the raw data using an in-house Python [32] pipeline. Briefly, the main steps consist of a signal-to-noise ratio peak picking procedure to filter the background signal, the intra-data (between pixels) and inter-data (between MSI runs) variabilities were then removed consecutively using peak alignment algorithms [33]. To reduce the effective data size, tissue-specific regions were semi-automatically identified [34,35] and peaks that were characterized as noisy or unlikely spatial distributions were removed using algorithms by means of the R package SPUTNIK [36]. A single data cube of dimension M x N was produced as output for each run, where M is the total number of pixels and N is the length of the common mass axis, which was shared between data from all runs.

To further reduce possible batch effect, the reference cores on each slide (i.e., kidney) were used to perform intensity scaling and finally the resulting data underwent median fold change scaling [37]. Total ion count images from each slide were co-registered with their corresponding H&E images, specifically by the use of affine transformation by gradient descent [22]. To enable supervised analysis, a clinical pathologist manually annotated cancerous tissue cores on the H&E optical images with clinicopathological information that allowed for more in-depth data mining.

To investigate the possible effect of sample age, cores from all available slides were grouped based on their respective collection years. The samples were grouped in 8 groups based on 10-year intervals of samples collected in 1940–2013. There was a clear bias towards certain year groups as the number of samples from each category ranged from 6 to 249 in this case. As such, a cost sensitive approach [38] was used to weight each group accordingly during model training. Additional groups were also tested based on 3-year, 5-year, 25-year, and 50-year sample intervals to further verify that the prediction results are not affected by the grouping. Weighted logistic regression (LR) classification models were built using Python and their performance assessed using leave-one-out-cross-validation between year groups. Model refinement by means of feature selection was then performed based on both univariate and multivariate statistical approaches. The pre-processed data cubes along with the year group labels were uploaded to MetaboAnalyst 5.0 (https://www.metaboanalyst.ca) [39] to undergo the Kruskal Wallis test. A threshold of ($p<0.05$) was used to select significantly different features in the intensity domain, which was followed by false discovery rate correction. In addition, the LR coefficients obtained from the cross-validated model were used as a measure of relative importance and the top 30 features for each 'one-vs-rest' case (i.e., 8 classes in total)

were extracted by ranking their absolute coefficient values. The unique features selected using this methodology were then compared with the univariate list. Overlapping features from the two approaches were ultimately considered features significantly affected by age for this study. Metabolic features were identified via literature search and online databases, including HMDB [40], Lipid maps [41], and Metlin [42].

3. Results

Access to FFPE samples spanning several decades enabled investigation into metabolite content over an unusually long period. The FFPE samples were grouped based on 10-year intervals ranging from 1940-2020, with the newest samples collected in 2013. Following this grouping, cost-sensitive logistic regression models were built, with the results illustrated in Fig. 1. The confusion matrix shows the performance of the model developed where an average classification accuracy of 96% was achieved. Further groupings were tested based on 3-year, 5-year, 25-year, and 50-year intervals with all showing similar average classification accuracies in the range of 96–98% (Supplementary Fig. 1A–D).

As the classification model indicates a clear dependence of data variation on sample age in this case, further investigation was carried out to determine the features that are involved in the differentiation. Using LR coefficients generated by the fitted model for each feature, which represent their relative weights and univariate analysis of variance, "important" features were extracted from the dataset. As such, a total of 152 features were deemed significant in separating the FFPE samples in terms of sample age. Using only these significant features, a new LR model was trained. To visualise the effect and validity of the feature selection process, Receiver Operator Characteristic (ROC) curve analysis was applied on the LR classification models before and after feature selection, where an overall macro-averaged ROC curve was obtained by averaging the individual curves for every class with equal weight. Fig. 2 thus shows that feature selection retained the model performance with the area-under-the-curve (AUC) changing from 0.98 to 0.97.

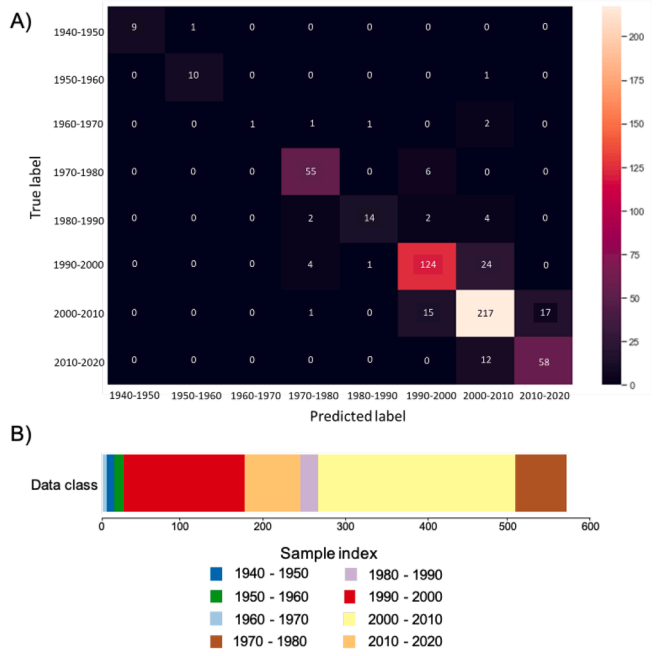

Fig. 1. Confusion matrix of the LR classification model produced by cross-validating the FFPE samples with 10-year interval ranging from the years 1940-2013, comparing the predicted age (x-axis) against the true age (y-axis), with true positives appearing along the matrix diagonal (A). The size of each group is also visualised and colour-coded to display the imbalance in distribution (B).

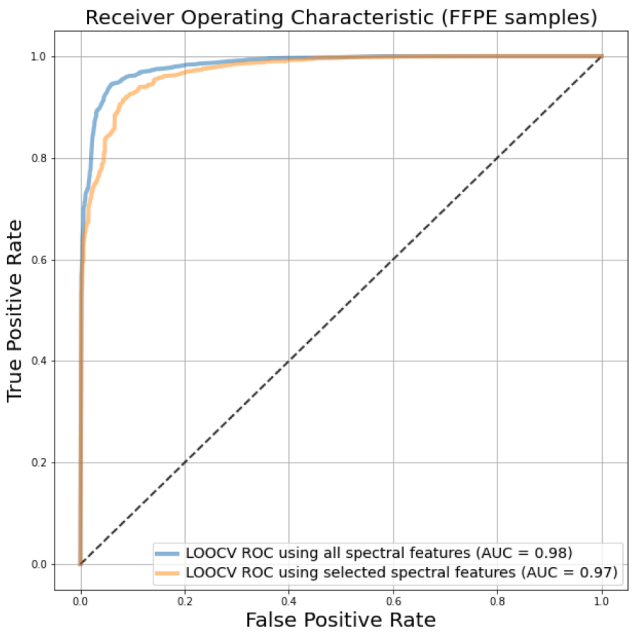

Fig. 2. Macro-averaged ROC curves for logistic regression models for FFPE samples. The blue line represents the model built using all spectral features and the orange line represents the model using only selected features deemed to be statistically significant.

Further examination of the pre-processed FFPE data revealed 326 histological specific features in total, with the signal intensities in the higher mass range (500–900 m/z) noticeably weaker than those in the lower mass range (100–500 m/z). We thus further investigated the mean intensities in these two regions separately as a function of time, which revealed a decrease in intensity for the low mass range (100–500 m/z), while higher mass range (500–900 m/z) features, including most lipids, were relatively stable (Fig. 3), suggesting an independence of sample age. Feature selection revealed 123 significant features detected in the lower mass range (see Supplementary Table 2). 87 features were detectable in the higher mass range, out of which 60 were found to be stable with respect to sample age via the process of feature selection. As FFPE samples underwent multiple solvent processing steps, FF samples were used to evaluate the validity of the 60 features for tissue analysis,

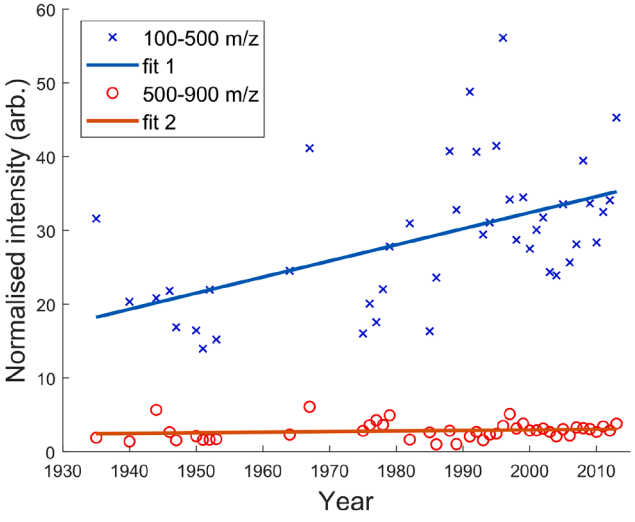

Fig. 3. The mean metabolic signal intensities of FFPE samples from the years 1935 - 2013. Blue crosses correspond to the lower mass range (100-500 m/z), while red dots correspond to the higher mass range (500-900 m/z). The solid lines represent the respective linear regressions performed on the data points.

giving a total of 7 features overlapping between FF and FFPE samples within a tolerance of 10 ppm. As an example, Fig. 4 displays the histological distribution of three features statistically unaffected by age and found in both FF TMA and FFPE TMA samples, whereas the list of all seven non-correlating and overlapping features can be found in Supplementary Table 3.

4. Discussion

Based on the classification results from the previous section, FFPE samples displayed clear separation when grouped by sample age. The cross-validated model thus successfully identified the correct sample age group with near perfect accuracy. Model optimisation by means of feature selection further retained this accuracy and yielded a list of the most significant features behind the intensity separation of different age groups. From the clear trend demonstrated in this representative dataset, there is an evident sample age dependence in terms of the mass spectral information, which was not removed by data pre-processing. This potentially signifies that any subsequent classification is also automatically influenced by this effect in features most affected. By careful annotation of the significant features obtained, several metabolically important features were highlighted. An example of which, taurine, has been widely discussed to be a potential biomarker for several diseases [18,20,43]. Taurine, however, is generally abundant in the human body and reliable biomarkers usually require a specific combination of multiple metabolites, whose intensities in the mass spectrum may be influenced non-uniformally by the effect of aging. In this regard, further investigation of metabolic spectral intensities (log-

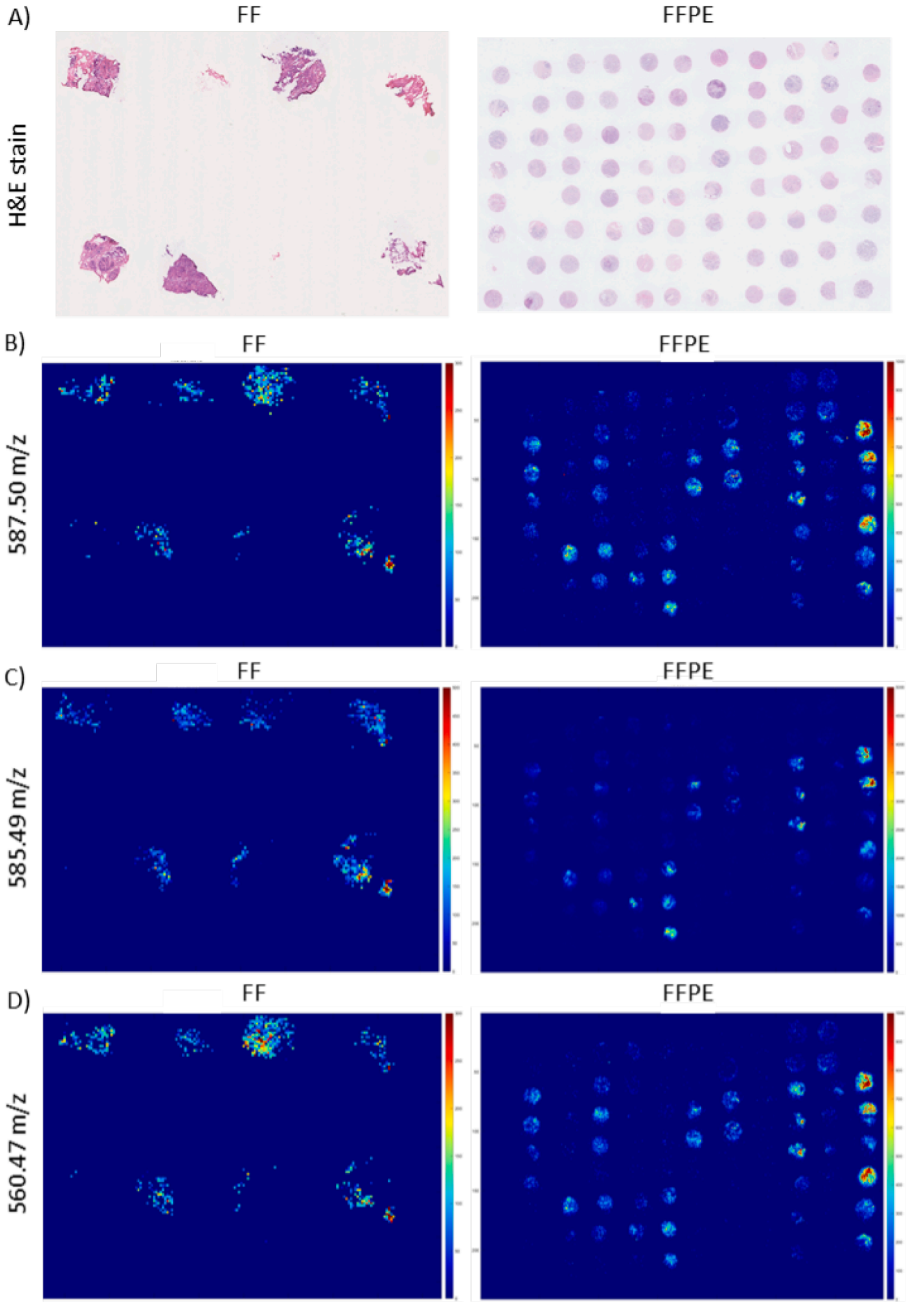

Fig. 4. Histological distribution of features of interest in one FF breast TMA and one FFPE breast TMA. To validate features from FFPE samples, ion images of the same features were explored in FF breast TMAs. A) H&E stain of FF TMA and FFPE TMA, B) Ion image of 587.50 m/z for FF TMA and FFPE TMA, C) Ion image of 585.49 m/z for FF TMA and FFPE TMA, D) Ion image of 560.47 m/z for FF TMA and FFPE TMA.

transformed) as a function of sample age was carried out by dividing the spectral range into low mass (100–500 m/z) and high mass (500–900 m/z) regions. It was found that the mean intensities (for every patient) in the low mass region decreased linearly as the samples aged, further validating the identification of certain distinguishing features such as taurine (m/z 124.0074). Linear regression performed on these data points produced a fit with a weak gradient of 0.218, hence displaying a direct, but weak, dependence on sample age with calculated F-statistics of 15.8 when null hypothesised against a constant model and a corresponding p-value of 2.76 e-4, indicating that the model is statistically significant within a confidence interval of 95%. On the other hand, the high mass region observed much lower mean intensities over the same time points, which is consistent with previous observations that deparaffinizing samples with solvents (e.g., xylene) removes lipid information that lies in this range [24]. Rather counter-intuitively, however, these intensities are more consistent with respect to sample age. A regression calculation in this case produced a low gradient (value) of 7.93 e-3 with the corresponding F-statistics and p-value at 1.08 and 0.305, respectively. This suggests that the null hypothesis that the data are constant in time cannot be rejected, thus statistically supporting the qualitative observation stated above. An apparent disadvantage of using FFPE samples for metabolic study is that the amount of solvent used in sample preparation reduces the lipid signal. Nonetheless, using matrix-assisted laser desorption ionisation mass spectrometry imaging (MALDI-MSI), several groups have shown that FFPE samples are appropriate for analytical purposes, with a 72% overlap of metabolites between FF and FFPE tissue [24,26,44]. Furthermore, our results suggest, despite their comparatively low intensities, features in the high mass region remained relatively constant over time. While solvent-resistant lipids have been reported to remain in FFPE tissue [45], these findings also hint at the auspicious possibility of using FFPE samples for meaningful metabolic analysis and diagnosis. In fact, the phosphatidylinositols (PI) PI (38:3), and PI (36:2) (887.56 m/z and 861.55 m/z) have been identified as potential biomarkers in breast cancer [16–18,46]. It should also be noted that the FF samples used as histological 'ground truth' in this case exhibit uncharacteristically low intensities in general, most probably due to their age, since the most recent sample was collected in 2003. The relatively low SNR is thus expected to introduce mass inaccuracies and may explain the sparsity in overlapping features with a stringent threshold of 10 ppm. Similarly, a few other overlapping features remain unidentified in this study, although further experimentation and perhaps comparative study with a dataset more representative in intensity can confirm their chemical species, as well as introducing more common features. In fact, inspired by this finding, our pilot study has also shown that FFPE samples could still be used to distinguish between normal and malignant tissues (unpublished data), demonstrating that the samples still contain sufficient biochemical information. This makes FFPE particularly interesting to study in the future given the plentiful and accessible nature of these kind of samples world-wide. With respect to the linear effect of sample age on low mass metabolites, this represents the well-documented issue of concept drift in machine learning [47]. Numerous approaches could be adopted to remedy the potential inaccuracy this may cause in predictive modelling. As demonstrated by the presented results, a simple linear relationship is expected from the effect of aging and such prior knowledge allows for the effective weighting of data from different age groups accordingly, although the weakness of the observed effect in this case may not pose serious difficulties even for a fixed model, which is consistent with some previous reports [24,25]. Alternatively, an ensemble approach is also possible where multiple models could be constructed from data of different ages, to avoid any overall bias towards any age group. Lastly, for the discovery of biomarkers, in particular, existing strategies often rely on the interplay and relative changes between a group of metabolites, which should stay consistent regardless of their individual intensity values. Specifically, the transformation of the intensity data into feature ratios should inherently remove this linear effect in the intensity domain.

5. Conclusions

The age of samples has long been hypothesised to affect the metabolic information contained within FFPE samples. In this work, the validity of this hypothesis was probed by means of supervised classification based on manual curation of FFPE samples into age groups. This is to our knowledge the first study of this kind showing the quantifiable impact of sample age on metabolic information in clinical samples as revealed by mass spectrometry imaging. Conversely, other factors such as possible changes in chemicals used in tissue processing over the years and solvents used in dewaxing the paraffin that are known to degrade metabolites will have to be considered for a truly quantitative analysis of said effect which sets the scene for future work. Overall, the FFPE samples appear to be affected weakly and linearly by sample age, especially in the low mass region, where the intensity of metabolites falls as the sample ages. On the other hand, albeit lower in intensity, the high mass region containing many useful lipid species retained stable signals over time, making FFPE samples a promising alternative for metabolic analysis in the future.

CRediT authorship contribution statement

Olof Gerdur Isberg: Conceptualization, Investigation, Formal analysis, Writing - original draft, Writing - review & editing, Visualization, Funding acquisition. **Yuchen Xiang:** Conceptualization, Formal analysis, Writing - original draft, Visualization, Writing - review & editing, Supervision. **Sigridur Klara Bodvarsdottir:** Conceptualization, Resources, Writing - review & editing, Supervision, Funding acquisition. **Jon Gunnlaugur Jonasson:** Validation, Resources, Writing - review & editing. **Margret Thorsteinsdottir:** Conceptualization, Writing - review & editing, Supervision, Funding acquisition. **Zoltan Takats:** Conceptualization, Writing - review & editing, Supervision.

Declaration of Conflicts of Interest

All authors declare that they have no known competing financial interests or personal relationships that could affect the work described in this article.

Appendix A. Supplementary data

Supplementary data associated with this article can be found, in the online version, athttps://doi.org/10.1016/j.jmsacl.2021.10.004.

References

[1] C.H. Johnson, J. Ivanisevic, G. Siuzdak, Metabolomics: beyond biomarkers and towards mechanisms, Nat. Rev. Mol. Cell Biol. 17 (July) (2016) 451–459.
[2] M.M. Rinschen, J. Ivanisevic, M. Giera, G. Siuzdak, Identification of bioactive metabolites using activity metabolomics, Nat. Rev. Mol. Cell Biol. 20 (6) (2019) 353–367, https://doi.org/10.1038/s41580-019-0108-4. ISSN 14710080.
[3] C.B. Clish, Metabolomics: an emerging but powerful tool for precision medicine, Mol. Case Stud. 1 (1) (2015), a000588, https://doi.org/10.1101/mcs.a000588. ISSN 2373-2865.
[4] E. Fahy, D. Cotter, M. Sud, S. Subramaniam, Lipid classification, structures and tools, Biochim. Biophys. Acta - Mol. Cell Biol, Lipids 1811 (11) (2011) 637–647, https://doi.org/10.1016/j.bbalip.2011.06.009. ISSN 13881981.
[5] N.L. Kuehnbaum, P. Britz-Mckibbin, New advances in separation science for metabolomics: Resolving chemical diversity in a post-genomic era, 2013, doi: 10.1021/cr300484s.
[6] X. Han, Lipidomics for studying metabolism, 2016, doi: 10.1038/nrendo.2016.98.
[7] T.A. Lydic, Y. Goo, Lipidomics unveils the complexity of the lipidome in metabolic diseases, Clin. Transl. Med. 7 (1), ISSN 2001–1326, doi: 10.1186/s40169-018-0182-9.
[8] T. Züllig, M. Trötzmüller, H.C. Köfeler, Lipidomics from sample preparation to data analysis: a primer, 2020, doi: 10.1007/s00216-019-02241-y.
[9] M.R. Wenk, The emerging field of lipidomics, Nat. Rev. Drug Discov. 4 (7) (2005) 594–610, https://doi.org/10.1038/nrd1776. ISSN 14741776.
[10] C.S. Clendinen, M.E. Monge, F.M. Fernández, Ambient mass spectrometry in metabolomics, Analyst 142 (17) (2017) 3101–3117, https://doi.org/10.1039/c7an00700k. ISSN 13645528.

[11] A.W. Fung, V. Sugumar, A.H. Ren, V. Kulasingam, Emerging role of clinical mass spectrometry in pathology, 2020, doi: 10.1136/jclinpath-2019-206269.
[12] Z. Tákats, J.M. Wiseman, B. Gologan, R.G. Cooks, Mass spectrometry sampling under ambient conditions with desorption electrospray ionization, Science (80-.). 306 (October) (2004) 471–473, doi: 10.1126/science.1104404.
[13] Z. Takáts, J.M. Wiseman, R.G. Cooks, Ambient mass spectrometry using desorption electrospray ionization (DESI): Instrumentation, mechanisms and applications in forensics, chemistry, and biology, J. Mass Spectrom. 40 (10) (2005) 1261–1275, https://doi.org/10.1002/jms.922. ISSN 10765174.
[14] P.M. Vaysse, R.M. Heeren, T. Porta, B. Balluff, Mass spectrometry imaging for clinical research-latest developments, applications, and current limitations, Analyst 142 (15) (2017) 2690–2712, https://doi.org/10.1039/c7an00565b. ISSN 13645528.
[15] N. Abbassi-Ghadi, K. Veselkov, S. Kumar, J. Huang, E. Jones, N. Strittmatter, H. Kudo, R. Goldin, Z. Takáts, G.B. Hanna, Discrimination of lymph node metastases using desorption electrospray ionisation-mass spectrometry imaging, Chem. Commun. 50 (28) (2014) 3661–3664, https://doi.org/10.1039/c3cc48927b. ISSN 1364548X.
[16] S. Guenther, L.J. Muirhead, A.V. Speller, O. Golf, N. Strittmatter, R. Ramakrishnan, R.D. Goldin, E. Jones, K. Veselkov, J. Nicholson, A. Darzi, Z. Takats, Spatially resolved metabolic phenotyping of breast cancer by desorption electrospray ionization mass spectrometry, Cancer Res. 75 (9) (2015) 1828–1837, https://doi.org/10.1158/0008-5472.CAN-14-2258. ISSN 15387445.
[17] A.M. Porcari, J. Zhang, K.Y. Garza, R.M. Rodrigues-Peres, J.Q. Lin, J.H. Young, R. Tibshirani, C. Nagi, G.R. Paiva, S.A. Carter, L.O. Sarian, M.N. Eberlin, L. S. Eberlin, Multicenter study using desorption-electrospray-ionization-mass-spectrometry imaging for breast-cancer diagnosis, Anal. Chem. 90 (19) (2018) 11324–11332, https://doi.org/10.1021/acs.analchem.8b01961. ISSN 15206882.
[18] A.L. Santoro, R.D. Drummond, I.T. Silva, S.S. Ferreira, L. Juliano, P.H. Vendramini, M.B. da Costa Lemos, M.N. Eberlin, V.P. Andrade, In situ Desi-MSI lipidomic profiles of breast cancer molecular subtypes and precursor lesions, Cancer Res. 80 (6) (2020) 1246–1257, ISSN 15387445, doi: 10.1158/0008-5472.CAN-18-3574.
[19] M.L. Dória, J.S. McKenzie, A. Mroz, D.L. Phelps, A. Speller, F. Rosini, N. Strittmatter, O. Golf, K. Veselkov, R. Brown, S. Ghaem-Maghami, Z. Takats, Epithelial ovarian carcinoma diagnosis by desorption electrospray ionization mass spectrometry imaging, Sci. Rep. 6, ISSN 20452322, doi: 10.1038/srep39219.
[20] M. Sans, K. Gharpure, R. Tibshirani, J. Zhang, L. Liang, J. Liu, J.H. Young, R. L. Dood, A.K. Sood, L.S. Eberlin, Metabolic markers and statistical prediction of serous ovarian cancer aggressiveness by ambient ionization mass spectrometry imaging, Cancer Res. 77 (11) (2017) 2903–2913, https://doi.org/10.1158/0008-5472.CAN-16-3044. ISSN 15387445.
[21] S. Gerbig, O. Golf, J. Balog, J. Denes, Z. Baranyai, A. Zarand, E. Raso, J. Timar, Z. Takats, Analysis of colorectal adenocarcinoma tissue by desorption electrospray ionization mass spectrometric imaging, Anal. Bioanal. Chem. 403 (8) (2012) 2315–2325, https://doi.org/10.1007/s00216-012-5841-x. ISSN 16182642.
[22] K.A. Veselkov, R. Mirnezami, N. Strittmatter, R.D. Goldin, J. Kinross, A.V. Speller, T. Abramov, E.A. Jones, A. Darzi, E. Holmes, J.K. Nicholson, Z. Takats, Chemo-informatic strategy for imaging mass spectrometry-based hyperspectral profiling of lipid signatures in colorectal cancer, Proc. Natl. Acad. Sci. U.S.A. 111 (3) (2014) 1216–1221, https://doi.org/10.1073/pnas.1310524111. ISSN 10916490.
[23] K. Arima, M.C. Lau, M. Zhao, K. Haruki, K. Kosumi, K. Mima, M. Gu, J.P. Väyrynen, T.S. Twombly, Y. Baba, K. Fujiyoshi, J. Kishikawa, C. Guo, H. Baba, W.G. Richards, A.T. Chan, R. Nishihara, J.A. Meyerhardt, J.A. Nowak, M. Giannakis, C.S. Fuchs, S. Ogino, Metabolic profiling of formalin-fixed paraffin-embedded tissues discriminates normal colon from colorectal cancer, Mol. Cancer Res. 18 (6) (2020) 883–890, https://doi.org/10.1158/1541-7786.MCR-19-1091. ISSN 15573125.
[24] A. Buck, A. Ly, B. Balluff, N. Sun, K. Gorzolka, A. Feuchtinger, K.P. Janssen, P. J. Kuppen, C.J. Van De Velde, G. Weirich, F. Erlmeier, R. Langer, M. Aubele, H. Zitzelsberger, M. Aichler, A. Walch, High-resolution MALDI-FT-ICR MS imaging for the analysis of metabolites from formalin-fixed, paraffin-embedded clinical tissue samples, J. Pathol. 237 (1) (2015) 123–132, https://doi.org/10.1002/path.4560. ISSN 10969896.
[25] S. Cacciatore, G. Zadra, C. Bango, K.L. Penney, S. Tyekucheva, O. Yanes, M. Loda, Metabolic profiling in formalin-fixed and paraffin-embedded prostate cancer tissues, Mol. Cancer Res. 15 (4) (2017) 439–447, https://doi.org/10.1158/1541-7786.MCR-16-0262. ISSN 15573125.
[26] A. Ly, A. Buck, B. Balluff, N. Sun, K. Gorzolka, A. Feuchtinger, K.P. Janssen, P. J. Kuppen, C.J. Van De Velde, G. Weirich, F. Erlmeier, R. Langer, M. Aubele, H. Zitzelsberger, L. McDonnell, M. Aichler, A. Walch, High-mass-resolution MALDI mass spectrometry imaging of metabolites from formalin-fixed paraffin-embedded tissue, Nat. Protoc. 11 (8) (2016) 1428–1443, https://doi.org/10.1038/nprot.2016.081. ISSN 17502799.
[27] N. Ogrinc, P.-D. Caux, Y.-M. Robin, E. Bouchaert, B. Fatou, M. Ziskind, C. Focsa, D. Bertin, D. Tierny, Z. Takats, M. Salzet, I. Fournier, Fast Cancer Molecular Diagnosis from FFPE Tissues Based on Metabolic Profiles Using SpiderMass Technology, SSRN Electron. J. ISSN 1556-5068, doi: 10.2139/ssrn.3732373.
[28] B. Donczo, A. Guttman, Biomedical analysis of formalin-fixed, paraffin-embedded tissue samples: The Holy Grail for molecular diagnostics, J. Pharm. Biomed. Anal. 155 (2018) 125–134, https://doi.org/10.1016/j.jpba.2018.03.065. ISSN 1873264X.
[29] J. Hermann, H. Noels, W. Theelen, M. Lellig, S. Orth-Alampour, P. Boor, V. Jankowski, J. Jankowski, Sample preparation of formalin-fixed paraffin-embedded tissue sections for MALDI-mass spectrometry imaging, Anal. Bioanal. Chem. 412 (6) (2020) 1263–1275, https://doi.org/10.1007/s00216-019-02296-x. ISSN 16182650.
[30] O.A. Stefansson, J.G. Jonasson, O.T. Johannsson, K. Olafsdottir, M. Steinarsdottir, S. Valgeirsdottir, J.E. Eyfjord, Genomic profiling of breast tumours in relation to BRCA abnormalities and phenotypes, Breast Cancer Res. 11 (4), ISSN 1465542X, doi: 10.1186/bcr2334.
[31] A. Dannhorn, E. Kazanc, S. Ling, C. Nikula, E. Karali, M.P. Serra, J.L. Vorng, P. Inglese, G. Maglennon, G. Hamm, J. Swales, N. Strittmatter, S.T. Barry, O. J. Sansom, G. Poulogiannis, J. Bunch, R.J. Goodwin, Z. Takats, Universal sample preparation unlocking multimodal molecular tissue imaging, Anal. Chem. 92 (16) (2020) 11080–11088, https://doi.org/10.1021/acs.analchem.0c00826. ISSN 15206882.
[32] G. Van Rossum, Python tutorial, Stichting Mathematisch Centrum, Amsterdam, The Netherlands, 1995. Tech. Rep.
[33] P. Inglese, H. Huang, V. Wu, M. Lewis, Z. Takats, Mass recalibration for desorption electrospray ionization mass spectrometry imaging using endogenous reference ions, 2021, doi: 10.1101/2021.03.29.437482.
[34] S. Klein, M. Staring, K. Murphy, M.A. Viergever, J.P. Pluim, Elastix: a toolbox for intensity-based medical image registration, IEEE Trans. Med. Imaging 29 (1) (2010) 196–205, https://doi.org/10.1109/TMI.2009.2035616. ISSN 02780062.
[35] D.P. Shamonin, E.E. Bron, B.P. Lelieveldt, M. Smits, S. Klein, M. Staring, Fast parallel image registration on CPU and GPU for diagnostic classification of Alzheimer's disease, Front. Neuroinform. 7 (JAN), ISSN 16625196, doi: 10.3389/fninf.2013.00050.
[36] P. Inglese, G. Correia, Z. Takats, J.K. Nicholson, R.C. Glen, SPUTNIK: An R package for filtering of spatially related peaks in mass spectrometry imaging data, Bioinformatics 35 (1) (2019) 178–180, https://doi.org/10.1093/bioinformatics/bty622. ISSN 14602059.
[37] K.A. Veselkov, L.K. Vingara, P. Masson, S.L. Robinette, E. Want, J.V. Li, R. H. Barton, C. Boursier-Neyret, B. Walther, T.M. Ebbels, I. Pelczer, E. Holmes, J. C. Lindon, J.K. Nicholson, Optimized preprocessing of ultra-performance liquid chromatography/mass spectrometry urinary metabolic profiles for improved information recovery, Anal. Chem. 83 (15) (2011) 5864–5872, https://doi.org/10.1021/ac201065j. ISSN 00032700.
[38] C.X. Ling, V.S. Sheng, Cost-sensitive learning and the class imbalance problem motivation and background, The University of Western Ontario, Canada, 2008. Tech. Rep.
[39] J. Xia, N. Psychogios, N. Young, D.S. Wishart, MetaboAnalyst: A web server for metabolomic data analysis and interpretation, Nucleic Acids Res. 37 (SUPPL. 2), ISSN 03051048, doi: 10.1093/nar/gkp356.
[40] D.S. Wishart, C. Knox, A.C. Guo, R. Eisner, N. Young, B. Gautam, D.D. Hau, N. Psychogios, E. Dong, S. Bouatra, R. Mandal, I. Sinelnikov, J. Xia, L. Jia, J.A. Cruz, E. Lim, C.A. Sobsey, S. Shrivastava, P. Huang, P. Liu, L. Fang, J. Peng, R. Fradette, D. Cheng, D. Tzur, M. Clements, A. Lewis, A. De souza, A. Zuniga, M. Dawe, Y. Xiong, D. Clive, R. Greiner, A. Nazyrova, R. Shaykhutdinov, L. Li, H.J. Vogel, I. Forsythei, HMDB: A knowledgebase for the human metabolome, Nucleic Acids Res. 37 (SUPPL. 1), ISSN 03051048, doi: 10.1093/nar/gkn810.
[41] K. Schmelzer, E. Fahy, S. Subramaniam, E.A. Dennis, The Lipid Maps Initiative in Lipidomics, 2007, doi: 10.1016/S0076-6879(07)32007-7.
[42] C.A. Smith, G. O'maille, E.J. Want, C. Qin, S.A. Trauger, T.R. Brandon, D.E. Custodio, R. Abagyan, G. Siuzdak, METLIN A Metabolite Mass Spectral Database, Ther Drug Monit 27 (6) (2005) 747–751, doi: 10.1097/01.ftd.0000179845.53213.39.
[43] D.Q. Chen, G. Cao, H. Chen, C.P. Argyopoulos, H. Yu, W. Su, L. Chen, D.C. Samuels, S. Zhuang, G.P. Bayliss, S. Zhao, X.Y. Yu, N.D. Vaziri, M. Wang, D. Liu, J.R. Mao, S. X. Ma, J. Zhao, Y. Zhang, Y.Q. Shang, H. Kang, F. Ye, X.H. Cheng, X.R. Li, L. Zhang, M.X. Meng, Y. Guo, Y.Y. Zhao, Identification of serum metabolites associating with chronic kidney disease progression and anti-fibrotic effect of 5-methoxytryptophan, Nat. Commun. 10 (1), ISSN 20411723, doi: 10.1038/s41467-019-09329-0.
[44] R. Casadonte, M. Kriegsmann, F. Zweynert, K. Friedrich, G. Bretton, M. Otto, S. O. Deininger, R. Paape, E. Belau, D. Suckau, D. Aust, C. Pilarsky, J. Kriegsmann, Imaging mass spectrometry to discriminate breast from pancreatic cancer metastasis in formalin-fixed paraffin-embedded tissues, Proteomics 14 (7–8) (2014) 956–964, https://doi.org/10.1002/pmic.201300430. ISSN 16159861.
[45] C. Hughes, L. Gaunt, M. Brown, N.W. Clarke, P. Gardner, Assessment of paraffin removal from prostate FFPE sections using transmission mode FTIR-FPA imaging, Anal. Methods 6 (4) (2014) 1028–1035, https://doi.org/10.1039/c3ay41308j. ISSN 17599660.
[46] J. Zhang, C.L. Feider, C. Nagi, W. Yu, S.A. Carter, J. Suliburk, H.S. Cao, L.S. Eberlin, Detection of metastatic breast and thyroid cancer in lymph nodes by desorption electrospray ionization mass spectrometry imaging, J. Am. Soc. Mass Spectrom. 28 (6) (2017) 1166–1174, https://doi.org/10.1007/s13361-016-1570-2. ISSN 18791123.
[47] A. Tsymbal, The problem of concept drift: definitions and related work, Trinity College Dublin, Ireland, 2004. Tech. Rep.